Theoretical Study of Nitrogen-Rich BeN_4 Compounds

Li Ping Cheng and Qian Shu Li*

State Key Lab of Prevention and Control of Explosion Disasters, School of Science, Beijing Institute of Technology, Beijing 100081, People's Republic of China

Received: June 2, 2003; In Final Form: November 11, 2003

Ab initio (MP2) and density functional theory (DFT) methods have been used to examine eight isomers of the singlet BeN_4 species with the 6-311+G* basis sets. The most stable isomer is the D_{2h} planar structure. Several decomposition and isomerization pathways for the BeN_4 species have been investigated. The D_{2h} planar, the C_{2v} branched, the C_s linear, and the C_{4v} pyramidal structures are all likely to be stable and to be observed experimentally due to their significant isomerizaion or dissociation barriers (20.9−125.3 kcal/mol). But the C_{2v} bent, the C_{2v} five-membered ring, and the C_{2v} cage structures are kinetically unstable. Among the known BeN_4 isomers, the C_s linear and the C_{4v} pyramidal structures are suitable to be potential high-energy-density materials (HEDMs) due to their high dissociation energies and significant dissociation or isomerization barriers.

1. Introduction

In recent years, polynitrogen compounds have been the subjects of intense theoretical and experimental scrutiny because of their potential use as high-energy-density materials (HEDMs).[1−12] However, their syntheses and handling have been great challenges for experimental chemists due to their metastable nature. The isolation of stable salts of the N_5^+ cation[13] has put the spotlight on the search for other stable polynitrogen species. Recently, Lee and Dateo[3] proposed that the most likely synthetic route for tetrahedral N_4 (Td N_4) arises from combination of two bound quintet states of N_2. Cacace et al.[14] prepared the tetranitrogen (N_4) from a linear $N_4^{\bullet+}$ radical cation and positively detected it as a gaseous metastable species with a lifetime exceeding 1 μs in experiments based on neutralization−reionization mass spectrometric (NRMS). More recently, Nguyen et al.[15] have determined the structures, stabilities, ionization, and neutralization of the tetranitrogen system related to the entire pathway occurring in the above NRMS procedure, and they found that the azidonitrene (N_3−N) is probably the N_4 molecule detected by Cacace et al. Vij et al.[16] reported the first experimental detection of the long-sought pentazole N_5^- anion by mass spectrometric techniques. These new discoveries indicate a bright future for experimental polynitrogen chemistry.

Besides theoretical interest in pure-nitrogen clusters, nitrogen-rich compounds have also attracted interest due to their potential use as HEDMs. Previously, Ferris and Bartlett[17] investigated theoretically the stability and vibrational properties of the pentazoles HN_5 using coupled-cluster (CC) and many-body perturbation theory (MBPT). Schleyer et al.[18] reported that the lithium salt, N_5Li, favors the planar C_{2v} structure containing dicoordinated lithium. Recently, Gagliardi and Pyykkö[19,20] have predicted the possible existence of two new class of compounds, Sc(η^7-N_7) and η^5-N_5^-− M−η^7-N_7^{3-} (M = Ti, Zr, Hf, and also Th). They pointed out that ScN_7 and N_5ThN_7 should have a fair chance of existing. Lein et al.[21] predicted the ferrocene-like Fe (η^5-N_5)$_2$ to be a strongly bonded complex with D_{5d} symmetry. Straka[22] performed a theoretical study on the possibility of stabilizing the N_6 species as a planar hexagonal ring in M(η_6-N_6) (M = Ti, Zr, Hf, Th) systems. Burke et al.[23] employed a theoretical characterization of pentazole anion with metal counterions, where the counterions considered are Na^+, K^+, Mg^{2+}, Ca^{2+}, and Zn^{2+}. Most recently, Wang et al.[24] have studied the stable structures of neutral, positive, and negative nitrogen-rich sulfides $(SN_3)_m$ (m = 1−4). We have investigated some nitrogen-rich compounds M_2N_4 (M = Li, Na, K, Rb, Cs),[25] and our computational results show that the bipyramidal M_2N_4 structures are likely to be stable and to be observed experimentally due to their significant isomerization or dissociation barriers (39.2−48.6 kcal/mol). The main purpose of the above theoretical investigations is to design nitrogen-rich compounds that store energy yet are stable enough for practical application as HEDMs.

Thompson et al.[26] have confirmed that it is possible to form beryllium nitrides by an experimental and theoretical study. They found that the reactions of pulsed-laser-ablated beryllium atoms with N_2 in argon and nitrogen matrixes could yield new beryllium−nitrogen species. To further identify the product molecules, they have done quantum chemical calculations. As a result, as shown in Figure 1, on the singlet surface, two possible BeN_4 structures were located at the RHF/6-311G* level of theory: the D_{2h} planar ^{1}**1** (N_2BeN_2) and the C_{2v} branched ^{1}**2** ($NNBeN_2$). Another two singlet BeN_4 structures were found at the MBPT(2)/6-311G* level of theory: the C_{2v} bent ^{1}**3** (NNBeNN), and the $D_{\infty h}$ linear ^{1}**4** (NNBeNN). On the triplet surface, the C_{2v} branched ^{3}**2** ($NNBeN_2$) were located at the ROHF/6-311G* level of theory. The C_{2v} bent ^{3}**3** (NNBeNN) and the C_{2v} quasi-linear ^{3}**4** (NNBeNN) were obtained at the ROHF/6-311G* and MBPT(2)/6-311G* levels of theory.[26] In their paper the authors have performed harmonic vibrational frequency calculations for most molecules. But to support the experimental results, they only listed the vibrational frequencies of one singlet species (^{1}**2**) and two triplet species (^{3}**3** and ^{3}**4**). Furthermore, the frequencies of ^{1}**2** and ^{3}**4** were calculated only at the Hartree−Fock level of theory. Thompson et al.[26] pointed out that the singlet ^{1}**2** is a local minimum but the triplet ^{3}**4** is a second-order saddle point. The triplet ^{3}**3** is a local minimum at the ROHF/6-311G* level of theory, but it is a first-order saddle point at the MBPT(2)/6-311G* level of theory.[26] Generally

* Corresponding author. Telephone: +86-10-6891-2665. Fax: +86-10-6891-2665. E-mail: qsli@bit.edu.cn.

10.1021/jp035536w CCC: $27.50
Published on Web 12/30/2003

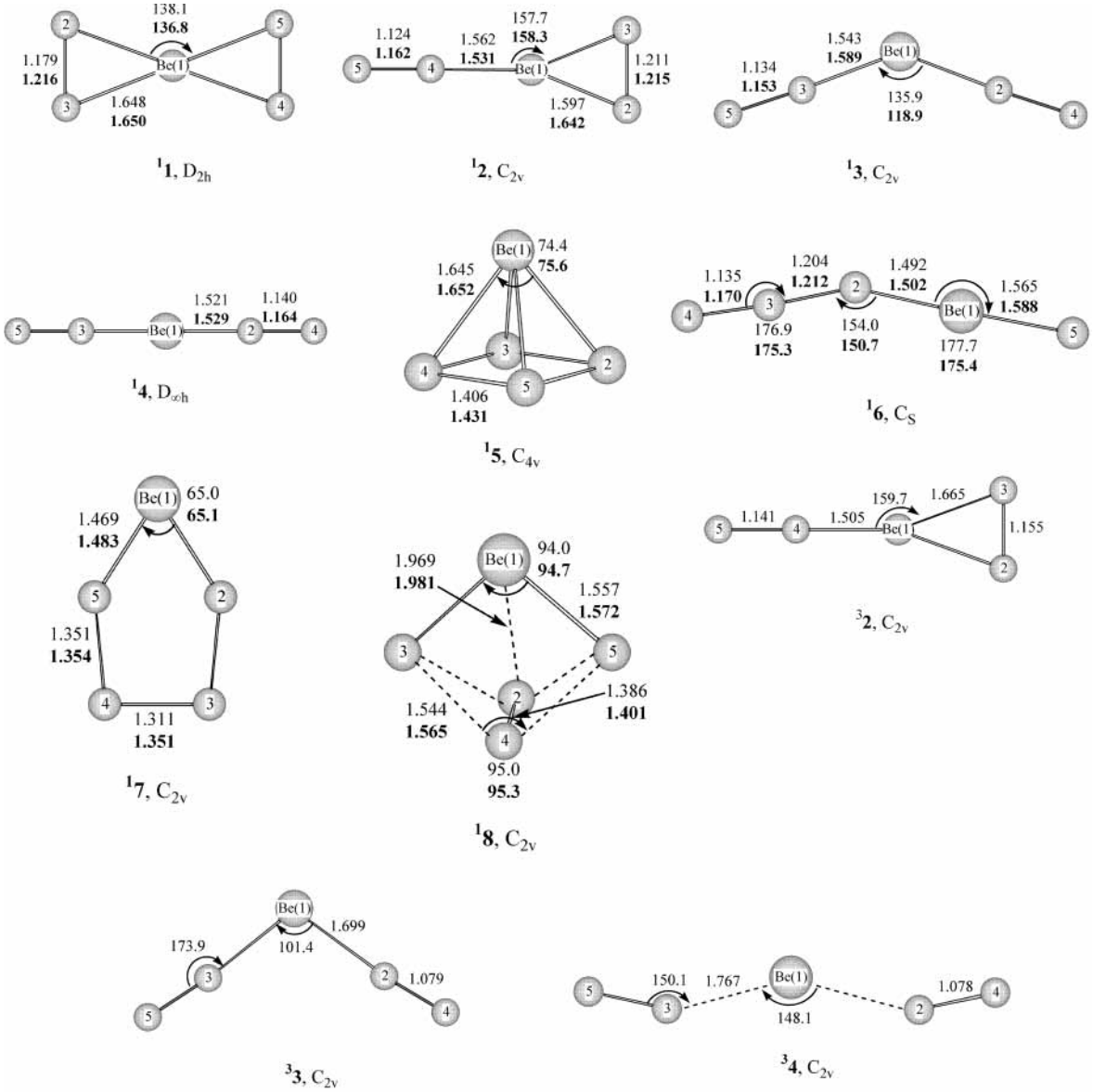

Figure 1. Optimized geometries for eight singlet and three triplet BeN_4 species reported by Thompson et al. at the B3LYP/6-311+G* and MP2/6-311+G* (bold font) levels of theory.

speaking, the results at the Hartree−Fock level are not very reliable due to the absence of electron correlation. On the other hand, although MP2 and MBPT(2) are the same level of electron correlation, it is necessary to further explore whether diffuse functions are important for the BeN_4 system. In addition, the energies provided by Thompson et al.[26] do not include the zero-point energy (ZPE) corrections, either. Therefore, it is necessary to use higher level, more expensive calculations for more accurate characterization of these novel molecular species.

In our ongoing work, we will continue to study BeN_4 compounds, and we expect to find new isomers. On the other hand, to our knowledge, no theoretical study has been devoted to the kinetic stabilities of the BeN_4 compounds.

It should be noted that our work in the present study focuses only on the singlet BeN_4 system. Further study on the corresponding triplet system is currently in progress and will be the subject of future publications.

2. Computational Methods

All calculations were performed using the Gaussian 98 program package.[27] We initially optimized geometries and calculated the harmonic vibrational frequencies for BeN_4 at the B3LYP/6-311+G* level of theory, where B3LYP is the DFT method using Becke's three-parameter gradient-corrected functional[28] with the gradient-corrected correlation of Lee, Yang, and Parr[29] and 6-311+G* is the split-valence triple-ζ plus polarization basis set augmented with diffuse functions.[30] Then, the geometries were refined and the vibrational frequencies were calculated at the level of second-order Møller−Plesset perturbation theory (MP2)[31] with the 6-311+G* basis set. Stationary points were characterized as minima without any imaginary vibrational frequency and a first-order saddle point with only one imaginary vibrational frequency. For transition states, the minimum energy pathways connecting the reactants and products were confirmed using the intrinsic reaction coordinate (IRC) method with the Gonzalez−Schlegel second-order algorithm.[32,33] Final energies were refined at the CCSD(T)[34]/6-311+G*//B3LYP/6-311+G* + ZPE (B3LYP/6-311+G*) level of theory.

Throughout this paper, bond lengths are given in angstroms, bond angles in degrees, total energies in hartrees, and relative and zero-point vibrational energies, unless otherwise stated, in kilocalories per mole.

TABLE 1: Total Energies (*E*),[a] Zero-Point Energies (ZPE),[b] and Relative Energies (RE)[c] for BeN_4 Species

	B3LYP/6-311+G*			MP2/6-311+ G*			CCSD(T)/6-311+G*//B3LYP/6-311+G*	
species	E[a]	ZPE[b]	RE[c]	E[a]	ZPE[b]	RE[c]	E[a]	RE[c]
^{1}**1** (D_{2h})	−233.792 17	10.3 (0)	0.0	−233.184 25	10.4 (0)	0.0	−233.212 49	0.0
^{1}**2** (C_{2v})	−233.795 03	10.4 (0)	−1.7	−233.172 30	9.9 (0)	7.0	−233.208 06	2.9
^{1}**3** (C_{2v})	−233.782 85	10.4 (0)	5.9	−233.159 64	9.8 (0)	14.8	−233.191 52	13.3
^{1}**4** ($D_{\infty h}$)	−233.782 30	10.7 (1)	6.6	−233.156 08	10.8 (1)	18.1	−233.190 41	14.3
^{1}**5** (C_{4v})	−233.641 22	11.8 (0)	96.2	−233.033 99	11.6 (0)	95.5	−233.058 24	98.3
^{1}**6** (C_s)	−233.640 99	10.7 (0)	95.3	−233.008 71	10.3 (0)	110.1	−233.051 71	101.3
^{1}**7** (C_{2v})	−233.616 51	11.6 (0)	111.5	−233.000 63	11.4 (0)	116.2	−233.027 42	117.4
^{1}**8** (C_{2v})	−233.584 77	9.5 (0)	129.3	−232.976 00	9.1 (0)	129.4	−233.008 82	127.0

[a] Total energies in hartrees. [b] Zero-point energies in kilocalories per mole. The integers in parentheses are the number of imaginary frequencies (NIMAG). [c] The relative energies with ZPE corrections in kilocalories per mole.

TABLE 2: Energies (au) for Several Singlet BeN_4 Species Reported by Thompson et al.

species	energy[a]	species	energy[b]
^{1}**1** (D_{2h})	−232.418 47	^{1}**3** (C_{2v})	−233.254 30
^{1}**2** (C_{2v})	−232.441 49	^{1}**4** ($D_{\infty h}$)	−233.254 36

[a] Energies at the RHF/6-311G* level of theory. [b] Energies at the restricted MBPT(2)/6-311G* level of theory.

3. Results and Discussion

Our optimized structures for eight singlet BeN_4 species are illustrated in Figure 1. Their total energies, ZPE, relative energies (with ZPE corrections), and number of imaginary frequencies are listed in Table 1. As is seen, except for the $D_{\infty h}$ linear structure, these BeN_4 isomers are all local minima on their potential energy surfaces (PES) at the above-mentioned two levels. For comparison, the total energies for structures ^{1}**1**−^{1}**4** provided by Thompson et al. are tabulated in Table 2. The optimized structures for nine transition states are shown in Figure 2. Their total energies, ZPE, and lowest vibrational frequencies are listed in Table 3. The energy differences between the minima and their corresponding transition states are tabulated in Table 4. The schematic potential energy surfaces for singlet BeN_4 isomers are depicted in Figure 3. The reaction energies for dissociation of the BeN_4 isomers to Be + $2N_2$ are shown in Table 5.

3.1. Structures and Stabilities of the BeN_4 Species. We performed ab initio calculations on a wide variety of singlet structures of BeN_4 by using two different and sophisticated theoretical methods. As exhibited in Figure 1, besides the reported four structures ^{1}**1**−^{1}**4**,[26] four new structures have been located, that is, the C_{4v} pyramidal ^{1}**5**, the C_S linear ^{1}**6**, the C_{2v} five-membered ring ^{1}**7**, and the C_{2v} cage ^{1}**8**. As seen from Table 1, according to our calculation, the energetic stability ordering of the eight isomers is ^{1}**1** > ^{1}**2** > ^{1}**3** > ^{1}**4** > ^{1}**5** > ^{1}**6** > ^{1}**7** > ^{1}**8** at the CCSD(T) level of theory. However, we found our results for isomers ^{1}**1**−^{1}**4** are different from those of Thompson et al. As shown in Table 2, Thompson et al.[26] reported that the D_{2h} planar ^{1}**1** is energetically higher than the C_{2v} branched ^{1}**2** by 14.4 kcal/mol (not including ZPE correction) at the RHF/6-311G* level of theory, and the energy (not including ZPE correction) of the C_{2v} bent ^{1}**3** is about equal to that of the $D_{\infty h}$ linear ^{1}**4** at the MBPT(2)/6-311G* level of theory. But, as mentioned above, the results at the RHF level are generally not very reliable. On the other hand, the two levels of MP2 and MBPT(2) are the same level of electron correlation and the difference between their computational results should mainly rely on the basis sets used. For example, according to Thompson et al.'s calculation, the structures of ^{1}**3** and ^{1}**4** have almost identical energies at the MBPT(2)/6-311G* level of theory. But, based on our computation, the C_{2v} bent ^{1}**3** is energetically lower than the $D_{\infty h}$ linear ^{1}**4** by 2.2 kcal/mol (not including ZPE correction) at the MP2/6-311+G* level of theory, indicating that diffuse functions are important for the singlet BeN_4 system.

As shown in Figure 1, it is apparent that the D_{2h} planar ^{1}**1** (N_2BeN_2) may be considered as a complex between the fragments of a beryllium atom and two equivalent dinitrogen molecules. Furthermore, the beryllium atom induces the lengthening in the N−N bond lengths (1.179−1.216 Å) from molecular nitrogen, suggesting that the interaction between Be and N atoms plays an important role in determining the geometry of species ^{1}**1**. The C_{2v} branched ^{2}**2** ($NNBeN_2$) is a local minimum of BeN_4 confirmed by Thompson et al.[26] Compared with the four bond lengths (N−$NBeN_2$, NN−BeN_2, Be−N (ring), and N−N (ring)), 1.070, 1.700, 1.516, and 1.236 Å (optimized at the RHF/6-311G* level) in Thompson et al.'s structure, our optimized bond lengths are 1.124, 1.562, 1.597, and 1.211 Å, respectively, at the B3LYP/6-311+G* level. The corresponding MP2 values are 1.162, 1.531, 1.642, and 1.215 Å, respectively. Infrared spectra identified that ^{1}**2** is a complex formed by a BeN_2 ring and a N_2 molecule.[26] As shown in Figure 1, the bond length of N4−N5, 1.124−1.162 Å, is indeed close to the experimental N≡N triple-bond length 1.098 Å for the nitrogen molecule N_2,[35] but the bond length of N2−N3, 1.211−1.215 Å, is more close to the double-bond length 1.252 Å of HN═NH.[35] Like the case in ^{1}**1**, the Be atom induces the lengthening in the N4−N5 bond from molecular nitrogen. We predict that structure ^{1}**1** is lower in energy than ^{1}**2** due to more N≡N triple bonds in structure ^{1}**1**. The covalent radius for nitrogen is 0.70 Å;[36] the corresponding value for Be is 0.89 Å.[36] Obviously, in structure ^{1}**1,** the Be−N bond distances (1.648−1.650 Å) are slightly longer than the sum of covalent radii of the corresponding Be atom and nitrogen atom. In structure ^{1}**2**, the Be1−N2 (N3) bond distances (1.597−1.642 Å) are also slightly longer than the sum of covalent radii of the corresponding Be atom and nitrogen atom, but the Be1−N4 bond distances (1.562−1.531 Å) are slightly shorter than the sum of covalent radii of the corresponding Be atom and nitrogen atom. To study the kinetic stabilities of these two isomers, their dissociation and isomerization reactions have been investigated. The schematic potential energy surfaces for isomers ^{1}**1** and ^{1}**2** are depicted in Figure 3. Structure **TS1** (seen in Figure 2) is a transition state (TS) of the dissociation of ^{1}**1** characterized to be a saddle point of index 1 by vibrational frequency analysis. IRC calculations performed at the B3LYP/6-311+G* and MP2/6-311+G* levels directly lead to dissociation into one Be atom and two N_2 molecules. The barrier for the decomposition reaction ^{1}**1** → **TS1** → Be + $2N_2$ is predicted to be 27.7 kcal/mol at the CCSD(T) level of theory, indicating the high kinetic stability toward decomposition. Similarly, structure **TS2** (C_s) is a transition structure of ^{1}**2** dissociating into Be + $2N_2$. The corresponding barrier was predicted to be 24.6 kcal/mol. The possible isomerization from ^{1}**1** to ^{1}**2** was

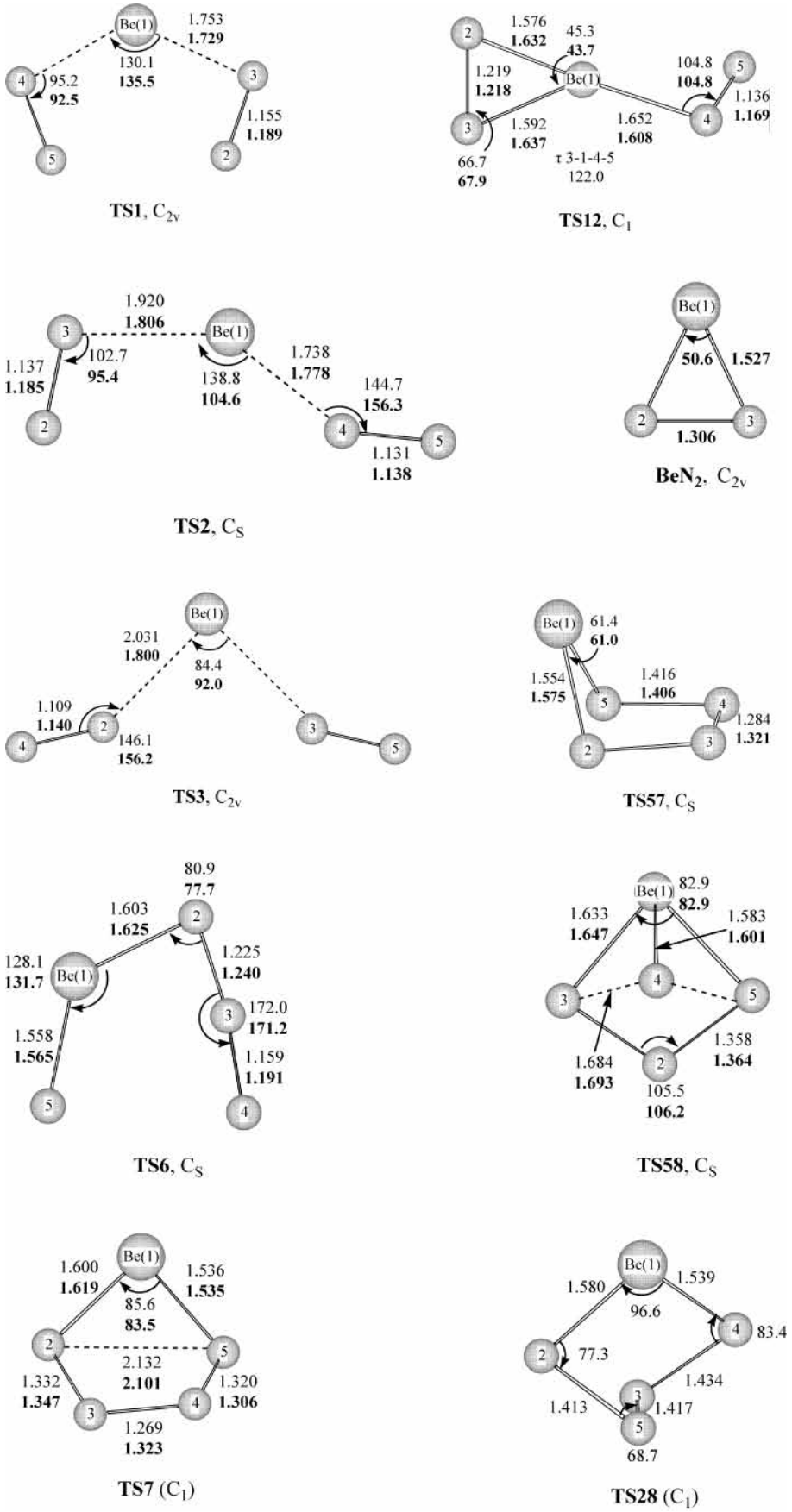

Figure 2. Optimized geometries for nine BeN_4 transition states and the cyclic BeN_2 species at the B3LYP/6-311+G* and MP2/6-311+G* (bold font) levels of theory.

also studied. The two conformers interconvert through a transition structure **TS12** (seen in Figure 2). Conformer ^{1}**1** converts to ^{1}**2** with a barrier of 25.2 kcal/mol, and conformer ^{1}**2** converts to ^{1}**1** with a barrier of 22.3 kcal/mol. Therefore,

TABLE 3: Total Energies (*E*) and Zero-Point Energies (ZPE) for the BeN_4 Transition States

species	B3LYP/6-311+G* E	B3LYP/6-311+G* ZPE[a]	MP2/6-311+G* E	MP2/6-311+G* ZPE[a]	CCSD(T)/6-311+G*//B3LYP/6-311+G* *E*
TS12 (C_1)	−233.756 47	9.5 (538*i*)[a]	−233.131 00	8.7 (678*i*)	−233.171 01
TS1 (C_{2v})	−233.742 34	9.0 (403*i*)	−233.137 31	8.7 (379*i*)	−233.166 30
TS2 (C_s)	−233.741 09	8.2 (388*i*)	−233.148 18	8.2 (283*i*)	−233.165 32
TS3 (C_{2v})	−233.765 40	8.2 (312*i*)	−233.156 89	7.9 (336*i*)	−233.204 29
TS57 (C_s)	−233.606 11	10.6 (311*i*)	−232.987 28	10.1 (284*i*)	−233.022 95
TS58 (C_s)	−233.535 29	9.1 (950*i*)	−232.912 07	9.6 (1089*i*)	−232.954 00
TS6 (C_s)	−233.592 04	10.1 (169*i*)	−232.966 35	10.0 (253*i*)	−233.004 98
TS7 (C_1)	−233.584 47	9.6 (994*i*)	−232.951 04	9.5 (1828*i*)	−233.018 60
TS28 (C_1)	−233.581 69	9.2 (250*i*)			−233.006 47

[a] The values in parentheses are the lowest vibrational frequencies [ν_1 (cm^{-1})].

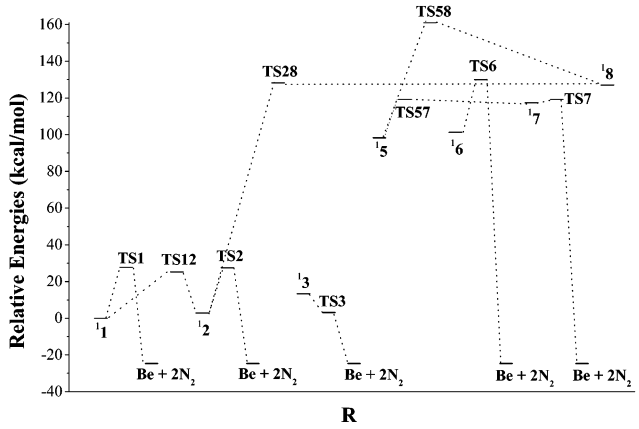

Figure 3. Schematic potential energy surfaces for singlet BeN_4 isomers.

TABLE 4: Energy Differences (kcal/mol) of Transition States Relative to BeN_4 Isomers (Including ZPE Corrections at the B3LYP/6-311+G* Level of Theory

species	B3LYP/ 6-311+G*	MP2/ 6-311+G*	CCSD(T)/6-311+G*// B3LYP/6-311+G*
^{1}**1** (D_{2h})	0.0	0.0	0.0
TS1 (C_{2v})	30.0	27.8	27.7
TS12 (C_1)	21.6	31.7	25.2
^{1}**2** (C_{2v})	0.0	0.0	0.0
TS2 (C_s)	31.6	13.4	24.6
TS12 (C_1)	23.3	24.7	22.3
TS28 (C_1)	132.7		125.3
^{1}**3** (C_{2v})	0.0	0.0	0.0
TS3 (C_{2v})	8.7	−0.2	−10.2
^{1}**5** (C_{4v})	0.0	0.0	0.0
TS57 (C_s)	20.8	27.8	20.9
TS58 (C_s)	63.8	74.5	62.7
^{1}**6** (C_s)	0.0	0.0	0.0
TS6 (C_s)	30.1	26.3	28.7
^{1}**7** (C_{2v})	0.0	0.0	0.0
TS7 (C_1)	18.1	29.2	3.5
TS57 (C_s)	5.5	7.1	1.8
^{1}**8** (C_{2v})	0.0	0.0	0.0
TS28 (C_1)	1.6		1.2
TS58 (C_s)	30.6	40.6	34.0

both species ^{1}**1** and ^{1}**2** possess significant kinetic stabilities toward isomerization.

Our kinetic analysis shows that these two isomers ^{1}**1** and ^{1}**2** are likely to be stable and to be observed experimentally.

The C_{2v} bent ^{1}**3** and the C_s linear ^{1}**6** are two chain structures. As tabulated in Table 1, they lie above ^{1}**1** by 13.3 and 101.3 kcal/mol at the CCSD(T) level of theory, respectively. As shown in Figure 1, the two terminal N−N bonds (1.134−1.153 Å) in structure ^{1}**3** are close to the N≡N triple bond (1.098 Å).[35] The bond lengths of N3−N4 (1.135−1.170 Å) in structure ^{1}**6** are also close to that of the N≡N triple bond, but the bond lengths of N2−N3 (1.204−1.212 Å) are closer to that of the N=N double bond (1.252 Å).[35] Structure ^{1}**3** is energetically lower than ^{1}**6** probably due to its more N≡N triple bonds. The Be−N distances in both ^{1}**3** and ^{1}**6** are slightly shorter than the sum of covalent radii of the corresponding Be atom and nitrogen atom. To further analyze their kinetic stabilities, we have investigated their decomposition pathways. The dissociation of ^{1}**3** proceeds in a straightforward manner with simple bond fissions. The transition state **TS3** (C_{2v}) was located on the PES. As shown in Figure 2, we note that, compared with structure ^{1}**3**, the two bond lengths of Be1−N2 and Be1−N3 in the transition state are stretched to eliminate two N_2 molecules, whereas those of N2−N4 and N3−N5 are actually compressed. The barrier for dissociation is only 8.7 kcal/mol at the B3LYP level and even negative at the MP2 and CCSD(T) levels. Such low barriers imply that structure ^{1}**3** is highly unstable toward decomposition. Similarly, structure **TS6** (C_s) is a dissociation transition structure of ^{1}**6**. IRC calculation performed at the B3LYP/6-311+G* level directly leads to dissociation into one Be atom and two N_2 molecules. The barriers for the decomposition reaction ^{1}**6** → **TS6** → Be + $2N_2$ are predicted to be 30.1 and 28.7 kcal/mol at the B3LYP and CCSD(T) levels of theory, respectively. However, IRC calculation performed at the MP2/6-311+G* level from **TS6** leads to BeN2 (C_{2v}), a planar cyclic structure (seen in Figure 2), and a N_2 molecule. The corresponding dissociation barrier is 26.3 kcal/mol. The moderate dissociation barriers suggest that species ^{1}**6** is stable kinetically.

TABLE 5: Reaction Energies (kcal/mol) for Dissociation of the BeN_4 Isomers to Be + $2N_2$

species	B3LYP/ 6-311+G*	MP2/ 6-311+G*	CCSD(T)/6-311+G*// B3LYP/6-311+G*
^{1}**1** (D_{2h})	2.4	15.2	24.7
^{1}**2** (C_{2v})	0.7	22.2	27.6
^{1}**3** (C_{2v})	8.3	30.0	38.0
^{1}**4** ($D_{\infty h}$)	9.0	33.3	38.9
^{1}**5** (C_{4v})	98.6	110.7	123.0
^{1}**6** (C_s)	97.6	125.2	126.0
^{1}**7** (C_{2v})	113.9	131.4	142.1
^{1}**8** (C_{2v})	131.7	144.6	151.7

Thompson et al.[26] had examined the $D_{\infty h}$ linear ^{1}**4** (NNBeNN) at the RHF and MBPT(2) levels of theory. But in their paper they did not provide the frequency calculation results for this isomer. According to our calculation, the singlet $D_{\infty h}$ linear ^{1}**4** is a first-order saddle point at both B3LYP and MP2 levels of theory. Due to its instability, less attention will be paid to it in the present study.

The C_{4v} pyramidal ^{1}**5**, the C_{2v} five-membered ring ^{1}**7**, and the C_{2v} cage ^{1}**8** are all high-energy species. They are higher in energy than the most stable ^{1}**1** by 98.3, 117.4, and 127.0 kcal/mol at the CCSD(T) level of theory, respectively. As shown in Figure 1, in structure ^{1}**5**, the N−N bond distances are all close to that of N−N single-bond and the Be−N distances are slightly longer than the sum of covalent radii of the corresponding Be atom and nitrogen atom. But, in structure ^{1}**7**, the case is different.

The bond distances between nitrogen and nitrogen are all between that of the N−N single-bond and the N═N double bond, and the Be−N distances are slightly shorter than the sum of covalent radii of the corresponding Be atom and nitrogen atom. Structure ^{1}**8** is interesting. Its lowest frequency (209 cm^{-1}) at the MP2/6-311+G* level is high enough to prove the minimum and corresponds to the nitrogen atoms rotating around the Be atom. As shown in Figure 1, the N−N bond distances in this structure are all either close to an N−N single bond or slightly longer, which is consistent with those in the Td N_4 (where all N−N linkages are single bonds). In structure ^{1}**8,** the Be1−N2 (N4) distances (1.969−1.981 Å) are far longer than the sum of covalent radii of the corresponding Be atom and nitrogen atom. While the Be1−N3 (N5) distances (1.557−1.572 Å) are slightly shorter than the sum of covalent radii of the corresponding Be atom and nitrogen atom. The schematic potential energy surfaces for isomers ^{1}**5**, ^{1}**7**, and ^{1}**8** are also depicted in Figure 3; indeed, on the basis of B3LYP and MP2 geometries, two transition structures (**TS57** and **TS58**, both with C_s symmetry) have been located connecting the pyramidal ^{1}**5** to other isomers on the PES. Clearly, structure **TS57** leads to the five-membered ring ^{1}**7**, whereas **TS58** connects ^{1}**5** and ^{1}**8**. The barrier going from ^{1}**5** to ^{1}**7** is 20.9 kcal/mol and from ^{1}**7** to ^{1}**5** is only 1.8 kcal/mol at the CCSD(T)/6-311+G*//B3LYP/6-311+G* + ZPE (B3LYP/6-311+G*) level of theory. The corresponding barrier from ^{1}**5** to ^{1}**8** is 62.7 kcal/mol and from ^{1}**8** to ^{1}**5** is 34.0 kcal/mol. Therefore, the rearrangements of ^{1}**5** and ^{1}**8** are difficult to occur, but species ^{1}**7** is not likely to be stable, and if it is formed in any process, it will transform into the pyramidal structure ^{1}**5**.

Possible decomposition mechanisms were studied for the pyramidal BeN_4 (^{1}**5**), in analogy with what was previously done for SrN_7,[19] by considering the opening of the nitrogen ring and locating the transition state (**TS7**) (Figure 2). **TS7** occurs when the N2−N5 bond opens to 2.101−2.132 Å. IRC calculations performed at the B3LYP and MP2 levels directly lead to dissociation into one Be and two N_2 molecules from **TS7**. However, IRC calculations confirmed that it is much more difficult to come back to the pyramidal ^{1}**5** than to the five-membered ring ^{1}**7** from **TS7**. Therefore, **TS7** is virtually the transition state for the decomposition of ^{1}**7** and the pyramidal ^{1}**5** is much more stable than ^{1}**7** with respect to decomposition. The energy barriers are calculated at 18.1 and 29.2 kcal/mol relative to ^{1}**7** at the B3LYP and MP2 levels of theory; single point calculation at the CCSD(T) level decreases this value to 3.5 kcal/mol. Such a low barrier implies that ^{1}**7** is quite unstable kinetically.

As shown in Figure 2, a transition structure **TS28** was located connecting the branched ^{1}**2** to the cage ^{1}**8** at the B3LYP/6-311+G* level of theory. The interconversion between ^{1}**2** and ^{1}**8** is characterized by an energy barrier of about 125.3 kcal/mol relative to ^{1}**2** and 1.2 kcal/mol relative to ^{1}**8**. Thus, species ^{1}**8** is highly unstable toward isomerization, and we need not further calculate its dissociation barrier to confirm its kinetic stability.

The reaction energies for dissociation of the BeN_4 isomers to Be + $2N_2$ molecules are listed in Table 5, and it appears that all reactions are exothermic. Furthermore, structures ^{1}**5** and ^{1}**6** have high dissociation energies as well as significant dissociation or isomerization barriers, and therefore should be regarded as suitable candidates for HEDMs.

4. Summary

We have examined eight nitrogen-rich BeN_4 compounds in the present study. Among them, the D_{2h} planar structure is the most energetically favored. Kinetic analysis shows that the D_{2h} planar, the C_{2v} branched, the C_s linear, and the C_{4v} pyramidal structures are all likely to be stable and to be observed experimentally. But the C_{2v} bent structure is kinetically unstable due to its low dissociation barrier. The C_{2v} five-membered ring and the C_{2v} cage structures are kinetically unstable with respect to isomeraization, and if they are formed in any process, they will transform into the C_{4v} pyramidal and the C_{2v} branched structures, respectively. Among the eight BeN_4 isomers, the C_s linear and the C_{4v} pyramidal structures may be possible to be used as HEDMs because of their high dissociation energies and significant dissociation or isomerization barriers.

References and Notes

(1) Glukhovtsev, M. N.; Jiao, H.; Schleyer, P. v. R. *Inorg. Chem.* **1996**, *35*, 7124.
(2) Lee, T. J.; Rice, J. E. *J. Chem. Phys.* **1991**, *94*, 1215.
(3) Lee, T. J.; Dateo, C. E. *Chem. Phys. Lett.* **2001**, *345*, 295.
(4) Lee, T. J.; Martin, J. M. L. *Chem. Phys. Lett.* **2002**, *357*, 319.
(5) Dunn, K. M.; Morokuma, K. *J. Chem. Phys.* **1995**, *102*, 4904.
(6) Francl, M. M.; Chesick, J. P. *J. Phys. Chem.* **1990**, *94*, 526.
(7) Engelke, R. *J. Phys. Chem.* **1992**, *96*, 10789.
(8) Bittererová, M.; Brinck, T. *J. Phys. Chem. A* **2000**, *104*, 11999.
(9) Gagliardi, L.; Orlandi, G.; Evangelisti, S.; Roos, B. O. *J. Chem. Phys.* **2001**, *114*, 10733.
(10) Tobita, M.; Bartlett, R. J. *J. Phys. Chem. A* **2001**, *105*, 4107.
(11) Leininger, M. L.; Sherrill, C. D.; Schaefer, H. F., III. *J. Phys. Chem.* **1995**, *99*, 2324.
(12) Chung, G.; Schmidt, M. W.; Gordon, M. S. *J. Phys. Chem. A* **2000**, *104*, 5647.
(13) Christe, K. O.; Wilson, W. W.; Sheehy J. A.; Boatz, J. A. *Angew. Chem., Int. Ed.* **1999**, *38*, 2004.
(14) Cacace, F.; Petris, G.; Troiani, A. *Science* **2002**, *295*, 480.
(15) Nguyen, M. T.; Nguyen, T. L., Mebel, A. M.; Flammang, R. *J. Phys. Chem. A* **2003**, *107*, 5452.
(16) Vij, A.; Pavlovich, J. G.; Wilson, W. W.; Vij, V.; Christe, K. O. *Angew. Chem., Int. Ed.* **2002**, *41*, 3051.
(17) Ferris, K. F.; Bartlett R. J. *J. Am. Chem. Soc.* **1992**, *114*, 8302.
(18) Glukhovtsev, M. N.; Schleyer, P. von. R.; Maerker, C. *J. Phys. Chem.* **1993**, *97*, 8200.
(19) Gagliardi, L.; Pyykkö, P. *J. Am. Chem. Soc.* **2001**, *123*, 9700.
(20) Gagliardi, L.; Pyykkö, P. *J. Phys. Chem. A* **2002**, *106*, 4690.
(21) Lein, M.; Frunzke, J.; Timoshkin, A.; Frenking, G. *Chem. Eur. J.* **2001**, *7*, 4155.
(22) Straka, M. *Chem. Phys. Lett.* **2002**, *358*, 531.
(23) Burke, L. A.; Butler, R. N.; Stephens, J. C. *J. Chem. Soc., Perkin Trans. 2* **2001**, *2*, 1679.
(24) Wang, L. J.; Zgierski, M. Z.; Mezey, P. G. *J. Phys. Chem. A* **2003**, *107*, 2080.
(25) Li, Q. S.; Cheng, L. P. *J. Phys. Chem. A* **2003**, *107*, 2882.
(26) Thompson, C. A.; Andrews, L.; Davy, R. D. *J. Phys. Chem.* **1995**, *99*, 7913.
(27) Frisch, M. J.; Trucks, G. W.; Schlegel, H. B.; Scuseria, G. E.; Robb, M. A.; Cheeseman, J. R.; Zakrzewski, V. G.; Montgomery, J. A., Jr.; Stratmann, R. E.; Burant, J. C.; Dapprich, S.; Millam, J. M.; Daniels, A. D.; Kudin, K. N.; Strain, M. C.; Farkas, O.; Tomasi, J.; Barone, V.; Cossi, M.; Cammi, R.; Mennucci, B.; Pomelli, C.; Adamo, C.; Clifford, S.; Ochterski, J.; Petersson, G. A.; Ayala, P. Y.; Cui, Q.; Morokuma, K.; Malick, D. K.; Rabuck, A. D.; Raghavachari, K.; Foresman, J. B.; Cioslowski, J.; Ortiz, J. V.; Stefanov, B. B.; Liu, G.; Liashenko, A.; Piskorz, P.; Komaromi, I.; Gomperts, R.; Martin, R. L.; Fox, D. J.; Keith, T.; Al-Laham, M. A.; Peng, C. Y.; Nanayakkara, A.; Gonzalez, C.; Challacombe, M.; Gill, P. M. W.; Johnson, B.; Chen, W.; Wong, M. W.; Andres, J. L.; Head-Gordon, M.; Replogle, E. S.; Pople, J. A. *Gaussian 98*, revision A.9; Gaussian, Inc.: Pittsburgh, PA, 1998.
(28) Becke, A. D. *J. Chem. Phys.* **1993**, *98*, 1372.
(29) Lee, C.; Yang, W.; Parr, R. G. *Phys. Rev. B* **1988**, *37*, 785.
(30) Hehre, W. J.; Radom, L.; Schleyer, P. v. R.; Pople, J. A. *Ab initio Molecular Orbital Theory*; Wiley: New York, 1986.
(31) Møller, C.; Plesset, M. S. *Phys. Rev.* **1934**, *46*, 618.
(32) Gonzalez, C.; Schlegel, H. B. *J. Chem. Phys.* **1989**, *90*, 2154.
(33) Gonzalez, C.; Schlegel, H. B. *J. Phys. Chem.* **1990**, *94*, 5523.
(34) Raghavachari, K.; Trucks, G. W.; Pople, J. A.; Head-Gordon, M. *Chem. Phys. Lett.* **1989**, *157*, 479.
(35) Lide, C. R. *CRC Handbook of Chemistry and Physics*, 73rd ed., CRC Press: Boca Raton, FL, 1992.
(36) http://chemed.chem.purdue.edu/genchem/topicreview/bp/ch7/size.html#cov.